NAVSEA
WARFARE CENTERS
NEWPORT

DEPARTMENT OF THE NAVY
NAVAL UNDERSEA WARFARE CENTER
DIVISION NEWPORT
OFFICE OF COUNSEL
PHONE: (401) 832-3653 FAX: (401) 832-4432
DSN: 432-3653

Attorney Docket No. 84709
Date: 5 July 2007

The below identified patent application is available for licensing. Requests for information should be addressed to:

PATENT COUNSEL
NAVAL UNDERSEA WARFARE CENTER
1176 HOWELL ST.
CODE 00OC, BLDG. 11
NEWPORT, RI 02841

Serial Number 11/772,280
Filing Date 2 July 2006

Inventor Andrew J. Hull

If you have any questions please contact James M. Kasischke, Supervisory Patent Counsel, at 401-832-4230.

DISTRIBUTION STATEMENT
Approved for Public Release
Distribution is unlimited

AN INVERSE METHOD TO CALCULATE MATERIAL PROPERTIES USING A NON-RESONANT TECHNIQUE

STATEMENT OF GOVERNMENT INTEREST

[0001] The invention described herein may be manufactured and used by or for the Government of the United States of America for governmental purposes without the payment of any royalties thereon or therefore.

BACKGROUND OF THE INVENTION

(1) Field of the Invention

[0002] The present invention relates to material properties measurement and, more particularly, to a method for measuring material properties using non-resonant techniques.

(2) Description of the Prior Art

[0003] Measuring the mechanical properties of slab-shaped (i.e., plates) materials are important because these parameters significantly contribute to the static and dynamic response of structures built with such materials. One characteristic that most elastomeric solids possess is that when they are subjected to large static forces (or pressure) their rigidity changes. Materials that have one set of mechanical properties at a

when subjected to increased pressure. The ability to determine the pressure dependence of material properties is extremely important for modeling the behavior of systems comprised of these materials.

[0004] Resonant techniques have been used to identify and measure longitudinal and shear properties for many years. These methods are based on comparing measured eigenvalues to modeled eigenvalues and calculating the resulting material properties. These methods do not account for static pressure or large compressive forces. Additionally, they typically require long, slender materials to perform the measurement process. Comparison of analytical models to measured frequency response functions is another method used to estimate stiffness and loss parameters of a structure. When the analytical model agrees with one or more frequency response functions, the parameters used to calculate the analytical model are considered accurate. If the analytical model is formulated using a numerical method, a comparison of the model to the data can be difficult due to dispersion properties of the materials. These methods do not take into account large compressive forces.

[0005] Some efforts have been made to measure material properties under large pressures. These methods consist of placing materials in pressurized settings, insonifying them, and then measuring their response. These methods are difficult

because they have to be conducted under great atmospheric pressure that can adversely effect the instrumentation. Safety issues can also arise in connection with laboratory testing at extreme pressures. Finally, a mass loaded long thin rod has been studied with respect to the bar wavespeed and corresponding Young's modulus. This work does not investigate shear motion.

[0006] Recently, a method to measure plate shaped materials subjected to large compressional forces was developed in U.S. Patent No. 6,848,311 incorporated by reference herein. This method is based on a single plate-shaped specimen and requires a graphical search routine to locate and estimate the propagation wavenumbers of the specimen.

SUMMARY OF THE INVENTION

[0007] One object of this invention is to accurately determine the material properties of a plate-shaped material specimen subjected to large static compressional forces.

[0008] The general purpose of this invention is to demonstrate a method to measure (or estimate) the complex frequency-dependent dilatational and shear wavenumbers of specimens subjected to large static compressional forces. The method uses two pieces of the same material where the thickness of the first piece is half the thickness of the second piece. This approach utilizes four transfer functions that are obtained

by vibrating both mass-loaded materials in two different directions, one vertical and one horizontal. Once this is accomplished, the transfer functions are combined with two theoretical models and then manipulated so that closed form equations which estimate the dilatational and shear wavenumbers as explicit functions of data and known system parameters are produced. The wavenumbers are then combined to determine complex dilatational wavespeed, complex shear wavespeed, complex Lamé constants, complex Young's modulus, complex shear modulus, and complex Poisson's ratio. This technique is described below.

[0009] This is an improvement to the previous method as it eliminates the need for a graphical search routine. Once these parameters have been estimated, the complex frequency-dependent dilatational and shear wavespeeds, Young's and shear moduli and Poisson's ratio can also be calculated. A typical test configuration is shown in FIGS. 1-2, where a test shaker initiates mechanical energy onto the plate-shaped specimen materials that are mass loaded. This approach is intended for use when the material is to be placed in an environment where it will be subjected to large pressure forces. This typically arises in submarines, where the panels that coat the exterior of the submarine are exposed to a wide range of hydrostatic pressures. An inverse method is developed using four transfer function measurements that are combined to yield closed form

equations of dilatational and shear wavenumbers at any given test frequency. Finally, dilatational and shear wavespeeds, Young's and shear moduli, and Poisson's ratio are then calculated.

BRIEF DESCRIPTION OF THE DRAWINGS

[0010] These and other features and advantages of the present invention will be better understood in view of the following description of the invention taken together with the drawings wherein :

[0011] **FIG. 1** is a diagram of a first test setup for the current invention;

[0012] **FIG. 2** is a diagram of a second test setup for the current invention;

[0013] **FIG. 3** is a diagram showing the coordinate system used by the current invention;

[0014] **FIGS. 4A** and **4B** are graphs of the transfer function for vertical motion and phase angle versus frequency;

[0015] **FIGS. 5A** and **5B** are graphs of the transfer function for horizontal motion and phase angle versus frequency;

[0016] **FIG. 6** is a plot of the function *s* versus frequency;

[0017] **FIGS. 7A** and **7B** are plots of the real and imaginary portion of the dilatational wavenumber versus frequency;

[0018] **FIG. 8** is a plot of the function *r* versus frequency;

[0019] **FIGS. 9A** and 9B are plots of the real and imaginary portions of the shear wavenumber versus frequency;

[0020] **FIGS. 10A** and **10B** are plots of the real and imaginary portions of Young's modulus versus frequency;

[0021] **FIGS. 11A** and **11B** are plots of the real and imaginary portions of shear modulus versus frequency; and

[0022] **FIG. 12** is a plot of the real part of Poisson's ratio versus frequency.

DETAILED DESCRIPTION OF THE INVENTION

[0023] The test procedure consists of vibrating a mass-loaded, slab-shaped test specimen **10** with a shaker **12** in two different directions, vertical **14A** and horizontal **14B**, as shown in **FIGS. 1** and **2**, respectively. It is noted that the mass 16 attached to the top of the material **10** must be sufficiently stiffer than the specimen **10** so that it can be modeled as lumped parameter expression rather than a continuous media system. A typical example would be steel attached above a rubber-like (or elastomeric) material giving a ratio of moduli of elasticity of greater than **100**. Lower ratios result in less accurate estimations. Vibrating the shaker **12** causes different waveforms to propagate in the material **10**. The inverse method developed here allows for the data from the experiments to be manipulated

so that the complex dilatational and shear wavenumbers can be measured. This test is usually done at multiple frequencies (swept sine) so any frequency dependencies can be identified and measured. Input vibration data is collected from the shaker **12**. A sensor **18** is mounted on load mass **16** and another sensor **20** is mounted on shaker **12** for collecting transfer function data. In **FIG. 1**, the test is set up for monitoring the vertical transfer function. **FIG. 2** shows the test as set up for monitoring the horizontal transfer function. Sensors **18** and **20** should be oriented properly to capture the motion being measured. Other test configurations using directions other than vertical and horizontal are possible; however, the test setups shown are preferred for ease of set up and calculation. These sensors **18** can be either accelerometers that record accelerations, or laser velocimeters that record velocities. In the swept sine mode, transfer functions of acceleration divided by acceleration or velocity divided by velocity are both equal to displacement divided by displacement. The time domain data collected from the sensors **18** and **20** are Fourier transformed into the frequency domain and then recorded as complex transfer functions, typically using a spectrum analyzer **22**.

[0024] In this method, different thicknesses h of material are used to calculate material properties of the specimen material **10**. Vertical and horizontal transfer functions are

obtained at thickness h = h_0. Vertical and horizontal transfer functions are also obtained at a second thickness where h = h_1 = $2h_0$. The coordinate system of the test configuration is shown in **FIG. 3**. Note that using this orientation results in b = 0 and a having a value less than zero. The thickness of the specimen, h, is a positive value.

[0025] For the single thickness shaker-specimen-mass system shown in **FIG. 1**, the transfer function between the vertical base displacement and the vertical mass displacement can be written as

$$T_1(\omega) = \frac{1}{R_1(\omega)} = \frac{U_z(0,b,\omega)}{U_0} = \frac{1}{\cos(k_d h) - \left(\frac{M}{\rho}\right) k_d \sin(k_d h)} \quad , \qquad (1)$$

where $T_1(\omega)$ or $R_1(\omega)$ correspond to the data from the vertical motion experiment using a single thickness specimen. In equation (1), M is the mass per unit area of the top mass (kg/m^2), ρ is the density of the test specimen (kg/m^3), h is thickness of the test specimen (m), and k_d is the dilatational wavenumber (rad/m) and is equal to

$$k_d = \frac{\omega}{c_d} \quad , \qquad (2)$$

where c_d is the dilatational wavespeed (m/s). For the double thickness shaker-specimen-mass system, the transfer function

between the vertical base displacement and the vertical mass displacement can be written as

$$T_2(\omega) = \frac{1}{R_2(\omega)} = \frac{U_z(0,b,\omega)}{U_0} = \frac{1}{\cos(2k_d h) - \left(\frac{M}{\rho}\right) k_d \sin(2k_d h)} \quad , \tag{3}$$

where $T_2(\omega)$ or $R_2(\omega)$ correspond to the data from the vertical motion experiment using a double thickness specimen. For the single thickness shaker-specimen-mass system shown in **FIG. 2**, the transfer function between the horizontal base displacement and the horizontal mass displacement can be written as

$$T_3(\omega) = \frac{1}{R_3(\omega)} = \frac{U_x(0,b,\omega)}{V_0} = \frac{1}{\cos(k_s h) - \left(\frac{M}{\rho}\right) k_s \sin(k_s h)} \quad . \tag{4}$$

where $T_3(\omega)$ or $R_3(\omega)$ correspond to the data from the horizontal motion experiment using a single thickness specimen. In equation (4), k_s is the shear wavenumber (rad/m) and is equal to

$$k_s = \frac{\omega}{c_s} \quad , \tag{5}$$

where c_s is the shear wavespeed (m/s). For the double thickness shaker-specimen-mass system shown in **FIG. 2**, the transfer function between the horizontal base displacement and the horizontal mass displacement can be written as

$$T_4(\omega) = \frac{1}{R_4(\omega)} = \frac{U_x(0,b,\omega)}{V_0} = \frac{1}{\cos(2k_s h) - \left(\frac{M}{\rho}\right) k_s \sin(2k_s h)} \quad . \tag{6}$$

where $T_4(\omega)$ or $R_4(\omega)$ correspond to the data from the horizontal motion experiment using a double thickness specimen. The dilatational wavespeed is related to the Lamé constants using the equation

$$c_d = \sqrt{\frac{\lambda + 2\mu}{\rho}} \tag{7}$$

and the relationship between the shear wavespeed and the Lamé constants is

$$c_s = \sqrt{\frac{\mu}{\rho}} \ , \tag{8}$$

where λ and μ are Lamé constants (N/m^2). The relationship of the Lamé constants to the Young's and shear moduli is shown as

$$\lambda = \frac{E\upsilon}{(1+\upsilon)(1-2\upsilon)} \tag{9}$$

and

$$\mu = G = \frac{E}{2(1+\upsilon)} \ , \tag{10}$$

where E is the complex Young's modulus (N/m^2), G is the complex shear modulus (N/m^2), and υ is the complex Poisson's ratio of the material (dimensionless).

[0026] The inverse solution for dilatational wavenumber can be determined by combining equations (1) and (3). A double angle trigonometric relationship is applied to both the sine and

cosine terms in equation (2), and the resulting equation is combined with equation (1) to yield

$$\cos(k_d h) = \frac{R_2 + 1}{2R_1} = \frac{T_1 + T_1 T_2}{2T_2} = \phi \quad , \tag{11}$$

where ϕ is a complex quantity. The inversion of equation (11) allows the complex dilatational wavenumber to be solved as a function of ϕ. The solution to the real part of k_d is

$$\mathrm{Re}(k_d) = \begin{cases} \dfrac{1}{2h}\mathrm{Arc}\cos(s) + \dfrac{n\pi}{2h} & n \text{ even} \\ \dfrac{1}{2h}\mathrm{Arc}\cos(-s) + \dfrac{n\pi}{2h} & n \text{ odd} \end{cases} \tag{12}$$

where

$$s = [\mathrm{Re}(\phi)]^2 + [\mathrm{Im}(\phi)]^2 - \sqrt{\left\{[\mathrm{Re}(\phi)]^2 + [\mathrm{Im}(\phi)]^2\right\}^2 - \left\{2[\mathrm{Re}(\phi)]^2 - 2[\mathrm{Im}(\phi)]^2 - 1\right\}} \quad , \tag{13}$$

n is a non-negative integer and the capital A denotes the principal value of the inverse cosine function. The value of n is determined from the function s, which is a cosine function with respect to frequency. At zero frequency, n is 0. Every time s cycles through π radians (180 degrees), n is increased by 1. When the solution to the real part of k_d is found, the solution to the imaginary part of k_d is then written as

$$\mathrm{Im}(k_d) = \frac{1}{h}\log_e\left\{\frac{\mathrm{Re}(\phi)}{\cos[\mathrm{Re}(k_d)h]} - \frac{\mathrm{Im}(\phi)}{\sin[\mathrm{Re}(k_d)h]}\right\} \quad . \tag{14}$$

[0027] The inverse solution for shear wavenumber can be determined by combining equations (4) and (6). A double angle trigonometric relationship is applied to both the sine and cosine terms in equation (6), and the resulting equation is combined with equation (4) to yield

$$\cos(k_s h) = \frac{R_4 + 1}{2R_3} = \frac{T_3 + T_3 T_4}{2T_4} = \theta \quad , \tag{15}$$

where θ is a complex quantity. The inversion of equation (11) allows the complex shear wavenumber to be solved as a function of θ. The solution to the real part of k_s is

$$\mathrm{Re}(k_s) = \begin{cases} \dfrac{1}{2h}\mathrm{Arccos}(r) + \dfrac{m\pi}{2h} & m \text{ even} \\ \dfrac{1}{2h}\mathrm{Arccos}(-r) + \dfrac{m\pi}{2h} & m \text{ odd} \end{cases} \tag{16}$$

where

$$r = [\mathrm{Re}(\theta)]^2 + [\mathrm{Im}(\theta)]^2 - \sqrt{\left\{[\mathrm{Re}(\theta)]^2 + [\mathrm{Im}(\theta)]^2\right\}^2 - \left\{2[\mathrm{Re}(\theta)]^2 - 2[\mathrm{Im}(\theta)]^2 - 1\right\}} \quad , \tag{17}$$

m is a non-negative integer and the capital A denotes the principal value of the inverse cosine function. The value of m is determined from the function r, which is a cosine function with respect to frequency. At zero frequency, m is 0. Every time r cycles through π radians (180 degrees), m is increased by 1. When the solution to the real part of k_s is found, the solution to the imaginary part of k_s is then written as

$$\mathrm{Im}(k_s) = \frac{1}{h}\log_e\left\{\frac{\mathrm{Re}(\theta)}{\cos[\mathrm{Re}(k_s)h]} - \frac{\mathrm{Im}(\theta)}{\sin[\mathrm{Re}(k_s)h]}\right\} \tag{18}$$

[0028] The material properties can be determined from the wavenumbers. First, the dilatational and shear wavespeeds are determined using

$$c_d = \frac{\omega}{k_d} \tag{19}$$

and

$$c_s = \frac{\omega}{k_s} \quad , \tag{20}$$

respectively. The Lamé constants are calculated using equations (7) and (8) written as

$$\mu = \rho c_s^2 \tag{21}$$

and

$$\lambda = \rho c_d^2 - 2\rho c_s^2 \quad . \tag{22}$$

Poisson's ratio is then calculated using

$$\upsilon = \frac{\lambda}{2(\mu+\lambda)} \quad . \tag{23}$$

Young's modulus can be calculated with

$$E = \frac{\mu(2\mu+3\lambda)}{(\mu+\lambda)} \tag{24}$$

and the shear modulus can be determined using

$$G \equiv \mu \quad . \tag{25}$$

[0029] The above measurement method can be simulated by means of a numerical example. Soft rubber-like material properties of the test specimen are used in this simulation. The material has a Young's modulus E of $[(1\times10^{8} - i2\times10^{7}) + (5\times10^{3}f - i3\times10^{2}f)]N/m^{2}$ where f is frequency in Hz, Poisson's ratio υ is equal to 0.40 (dimensionless), density ρ is equal to 1200 kg/m^{3}, and a thicknesses h of 0.1 m and 0.2 m. The top mass is a 0.0254 m (1 inch) steel plate that has a mass per unit area value M of 199 kg/m^{2}. **FIG. 4A** is a plot of the transfer function of the systems for vertical motion versus frequency and corresponds to equation (1) and (3). **FIG. 4B** is a plot of the phase angle of the systems motion. **FIGS. 5A** and **5B** are plots of the transfer function of the systems for horizontal motion versus frequency and corresponds to equations (4) and (6). In **FIGS. 4A** and **5A** the motion plots have magnitude in decibels, and **FIGS. 4B** and **5B** show the phase angle in degrees.

[0030] **FIG. 6** is a plot of the function s versus frequency and corresponds to equation (13). The values for the indices n and the corresponding frequencies can be determined from the inspection of FIG. 6 and are listed in Table 1.

Table 1. The Value of *n* Versus Frequency

n	Minimum Frequency (Hz)	Maximum Frequency (Hz)
0	0	1100
1	1100	2257
2	2257	3476
3	3476	4753
4	4753	5000

[0031] **FIGS. 7A** and **7B** are plots of the real and imaginary portion of the dilatational wavenumber versus frequency. In both plots, the solid line is the actual wavenumber used to formulate the model and the x markers are the estimated values of the real and imaginary wavenumbers determined using equations (12) and (14), respectively. **FIG. 8** is a plot of the function *r* versus frequency and corresponds to equation (17). The values for the indices *m* and the corresponding frequencies can be determined from the inspection of **FIG. 8** and are listed in Table 2.

Table 2. The Value of *m* Versus Frequency

m	Minimum Frequency (Hz)	Maximum Frequency (Hz)
0	0	442
1	442	894
2	894	1355
3	1355	1826
4	1826	2306
5	2306	2797
6	2797	3297
7	3297	3808
8	3808	4330
9	4330	4862
10	4753	5000

[0032] **FIGS. 9A** and **9B** are plots of the real and imaginary portions of the shear wavenumber versus frequency. In both plots, the solid line is the actual wavenumber used to formulate the model and the + markers are the estimated values of the real and imaginary wavenumbers determined using equations (16) and (18), respectively.

[0033] **FIGS. 10A** and **10B** are plots of the real and imaginary portions of Young's modulus versus frequency. In both plots,

the solid line is the actual modulus used to formulate the model and the + markers are the estimated values of real and imaginary Young's modulus determined using equations (19) through (22) and (24). **FIG. 11A** and **11B** are plots of the real and imaginary portions of shear modulus versus frequency. In both plots, the solid line is the actual modulus used to formulate the model and the x markers are the estimated values of real and imaginary shear modulus determined using equations (19) through (22) and (25). **FIG. 12** is a plot of the real part of Poisson's ratio versus frequency. The solid line is the actual ratio used to formulate the model and the square markers are the estimated values of the real part of Poisson's ratio determined using equations (19) through (23). Because the numerical example is formulated using a Poisson's ratio that is strictly real, no imaginary component is shown in this plot. Imaginary values of Poisson's ratio are possible and have been shown to theoretically exist.

[0034] This method provides many new features and advantages. It gives the ability to estimate the complex dilatational and shear wavespeeds of a material that is slab-shaped and subjected to compressive forces with closed form expressions. It also allows estimation of the complex Lamé constants of a material that is slab-shaped and subjected to compressive forces with closed form expressions. Other parameters can also be estimated

with closed form expressions such as the complex Young's and shear moduli, and complex Poisson's ratio.

[0035] In light of the above, it is therefore understood that within the scope of the appended claims, the invention may be practiced otherwise than as specifically described.

ABSTRACT OF THE DISCLOSURE

A method for calculating material properties of a material includes determining a dilatational wavespeed and a shear wave speed. The dilatational wavespeed is determined by conducting vertical vibration tests of two specimens of the material, one specimen being twice as thick as the other. Transfer functions are obtained from these tests and used to calculate the dilatational wavespeed. The shear wavespeed is determined by conducting horizontal vibration tests of two specimens with one specimen being twice as thick as the other. The shear wavespeed can be calculated from transfer functions obtained from these tests and the dilatational wavespeed. Other material properties can be calculated from the dilatational and shear wavespeeds. Frequency dependence of the properties can be determined by conducting the tests at different frequencies.

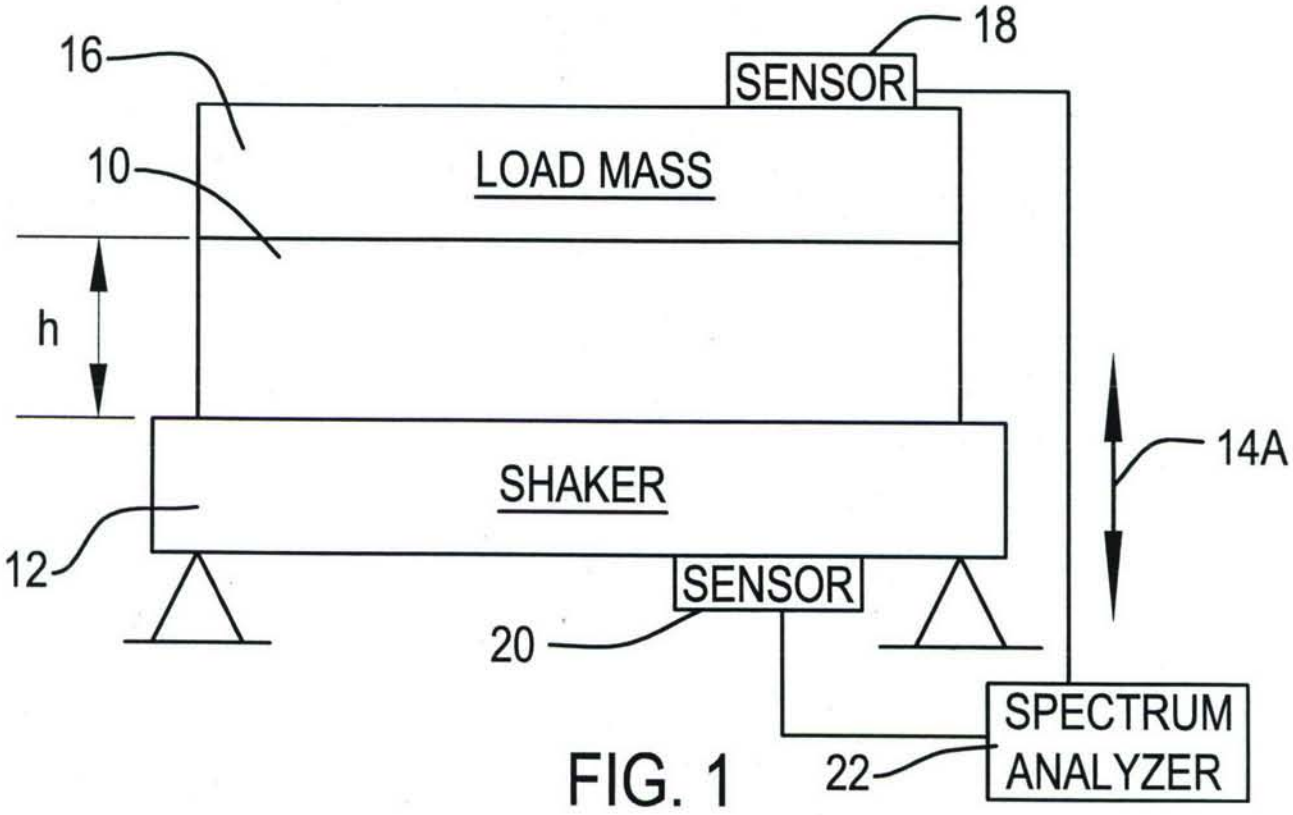
16
18
SENSOR
10
LOAD MASS
h
14A
SHAKER
12
SENSOR
20
SPECTRUM
ANALYZER
22

FIG. 1

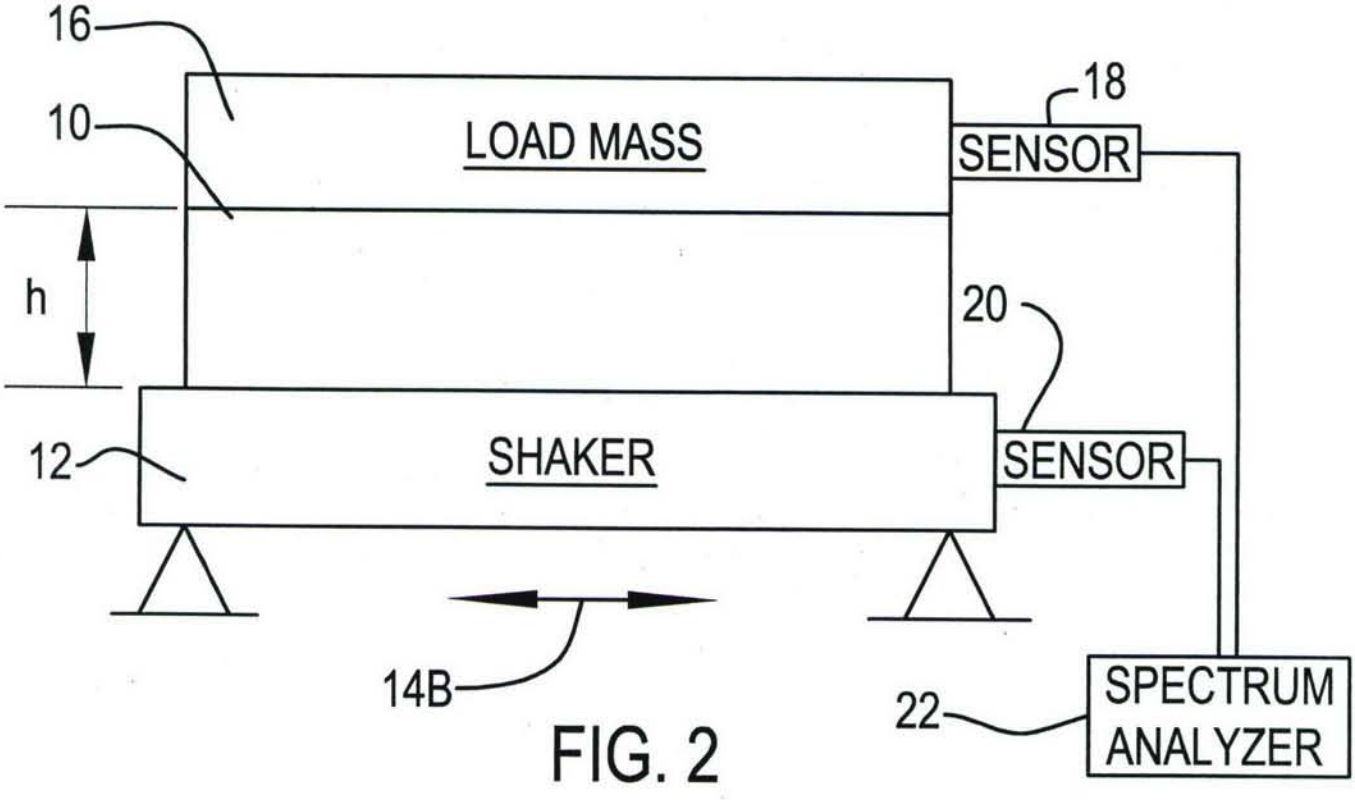
16
18
10
LOAD MASS
SENSOR
h
20
12
SHAKER
SENSOR
14B
SPECTRUM
ANALYZER
22

FIG. 2

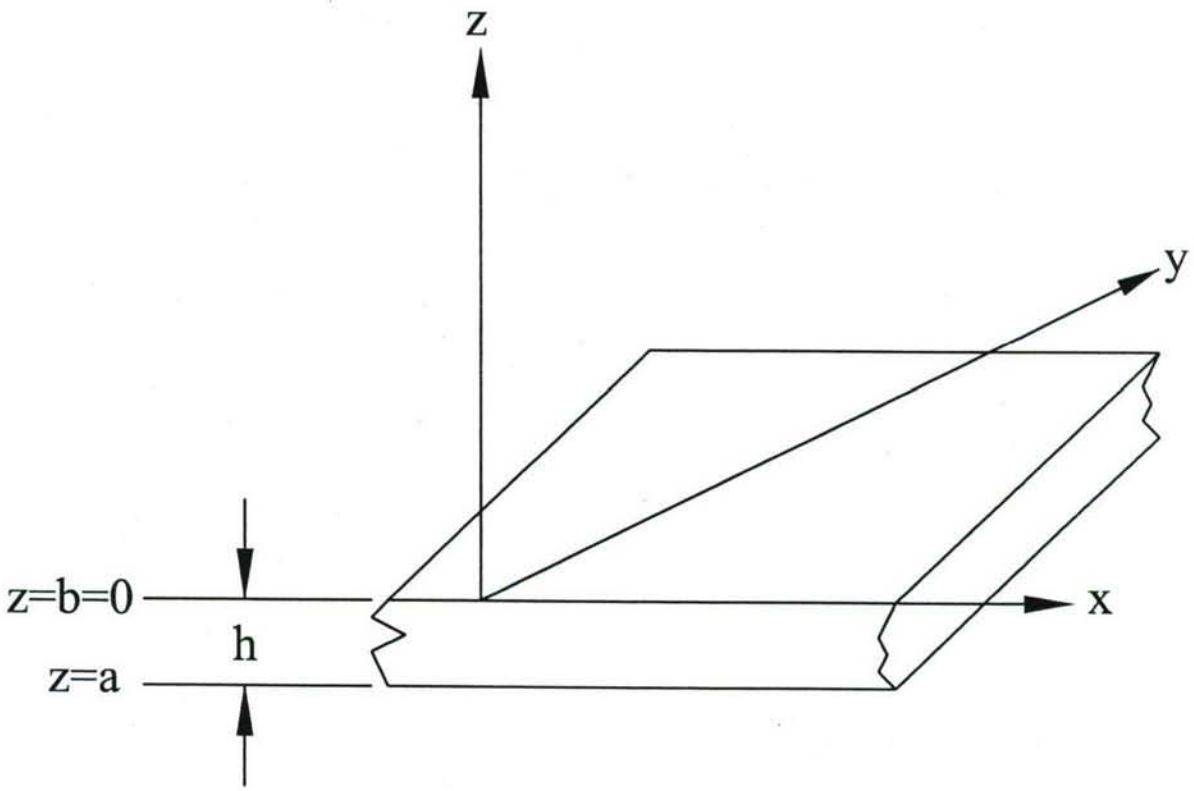

FIG. 3

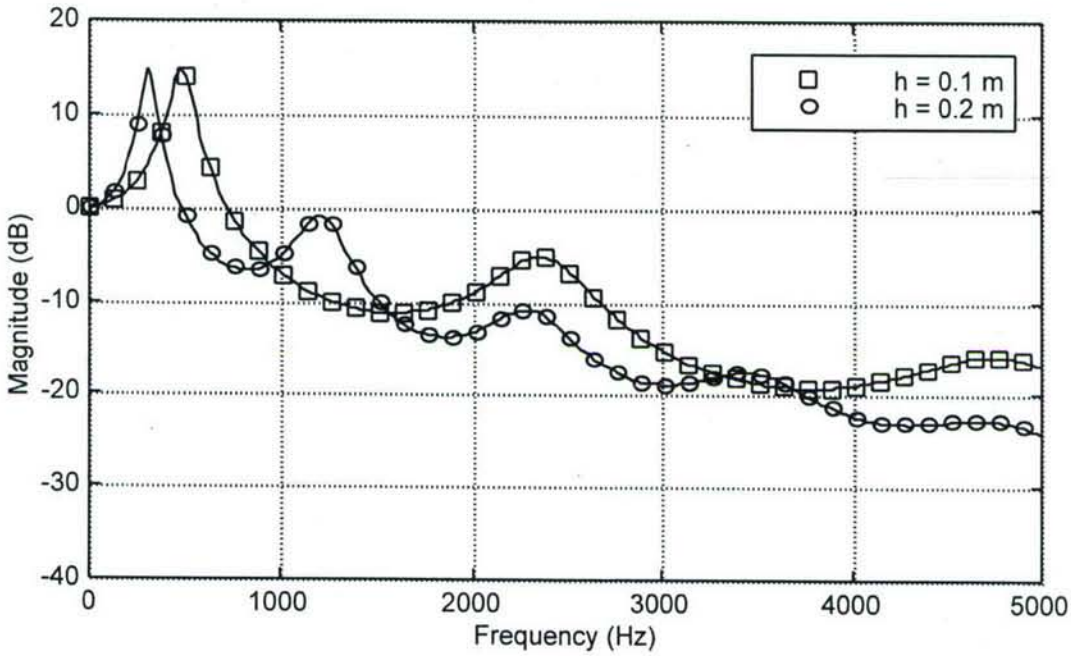
h = 0.1 m
h = 0.2 m
Magnitude (dB)
Frequency (Hz)
20
10
0
-10
-20
-30
-40
0
1000
2000
3000
4000
5000

FIG. 4A

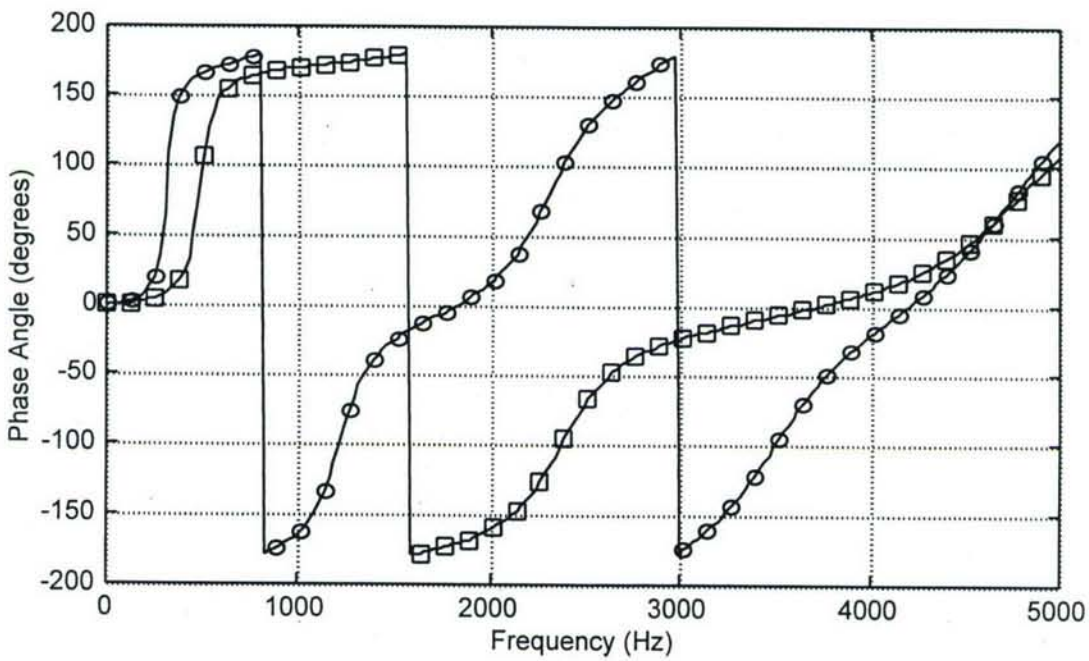
Phase Angle (degrees)
Frequency (Hz)
200
150
100
50
0
-50
-100
-150
-200
0
1000
2000
3000
4000
5000

FIG. 4B

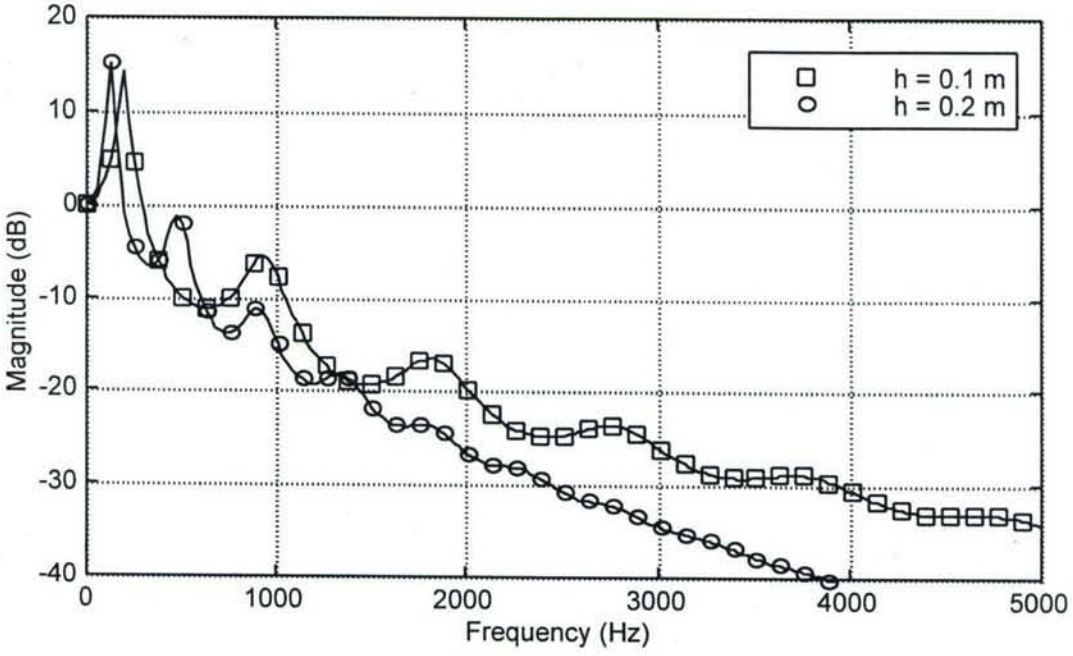
h = 0.1 m
h = 0.2 m
Magnitude (dB)
Frequency (Hz)
20
10
0
-10
-20
-30
-40
0
1000
2000
3000
4000
5000

FIG. 5A

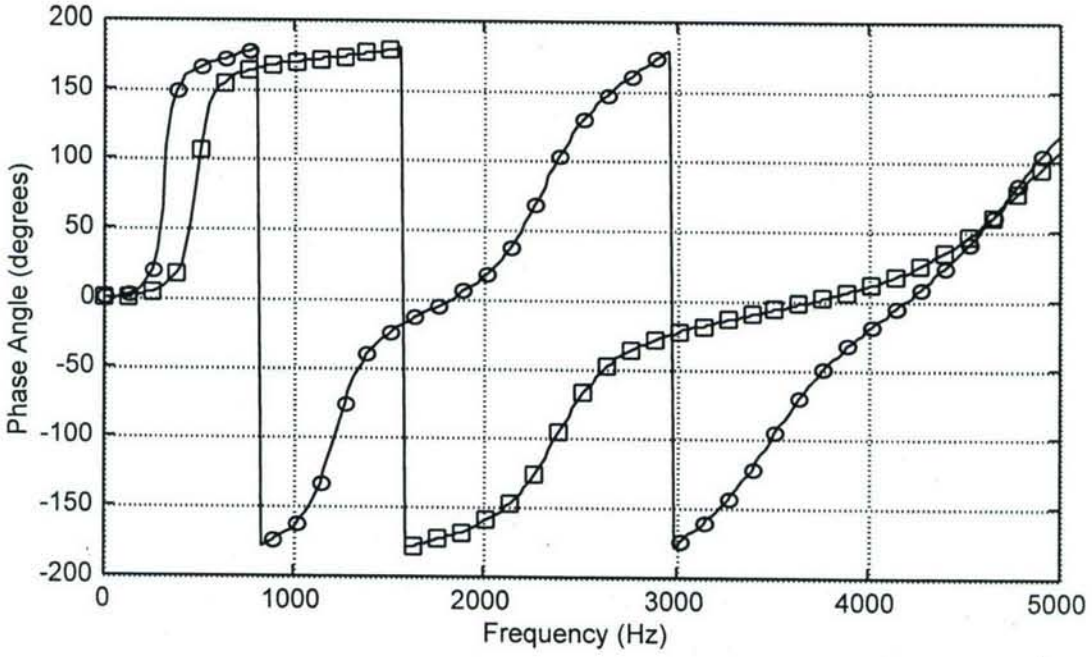
Phase Angle (degrees)
Frequency (Hz)
200
150
100
50
0
-50
-100
-150
-200
0
1000
2000
3000
4000
5000

FIG. 5B

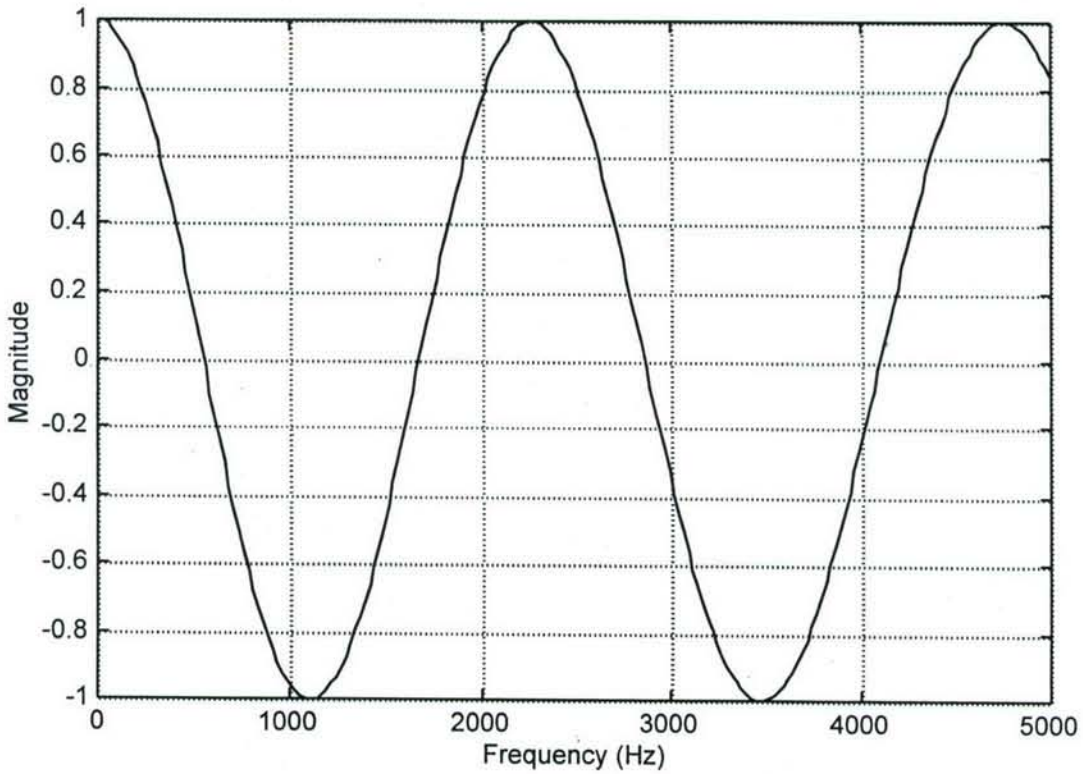
1
0.8
0.6
0.4
0.2
0
-0.2
-0.4
-0.6
-0.8
-1
Magnitude
0
1000
2000
3000
4000
5000
Frequency (Hz)

FIG. 6

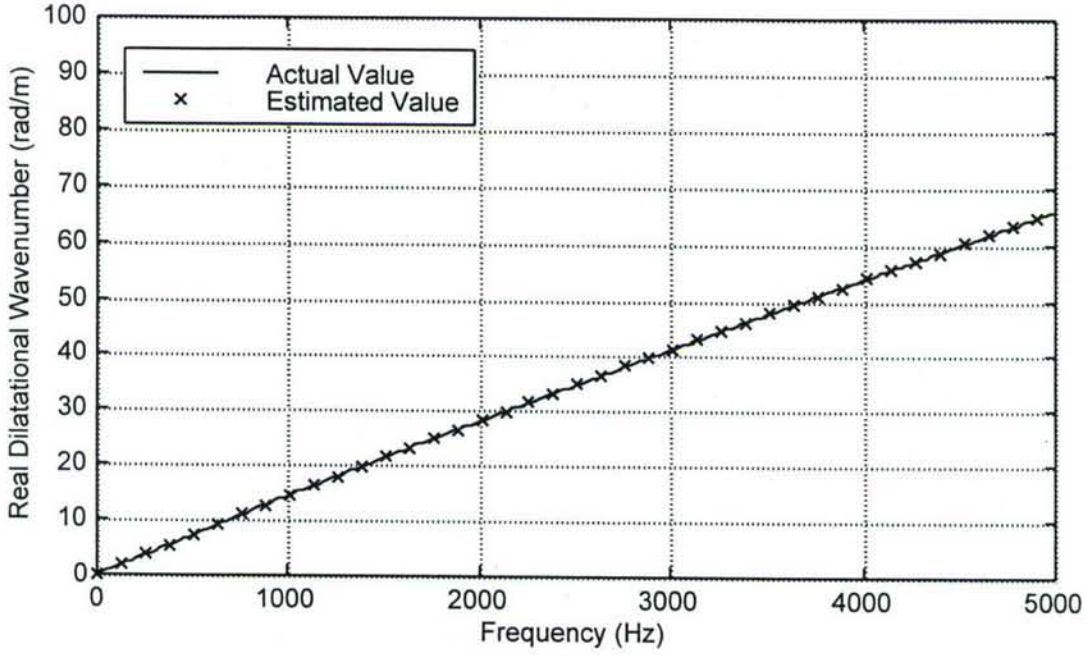
Actual Value
Estimated Value
Real Dilatational Wavenumber (rad/m)
Frequency (Hz)
0
10
20
30
40
50
60
70
80
90
100
0
1000
2000
3000
4000
5000

FIG. 7A

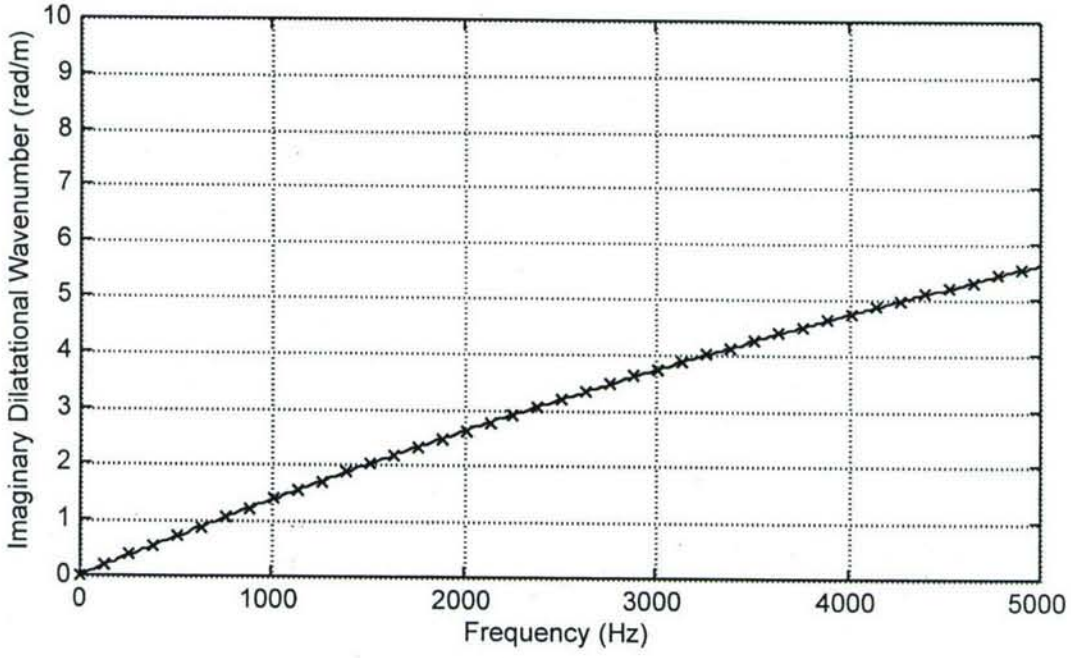
Imaginary Dilatational Wavenumber (rad/m)
Frequency (Hz)
0
1
2
3
4
5
6
7
8
9
10
0
1000
2000
3000
4000
5000

FIG. 7B

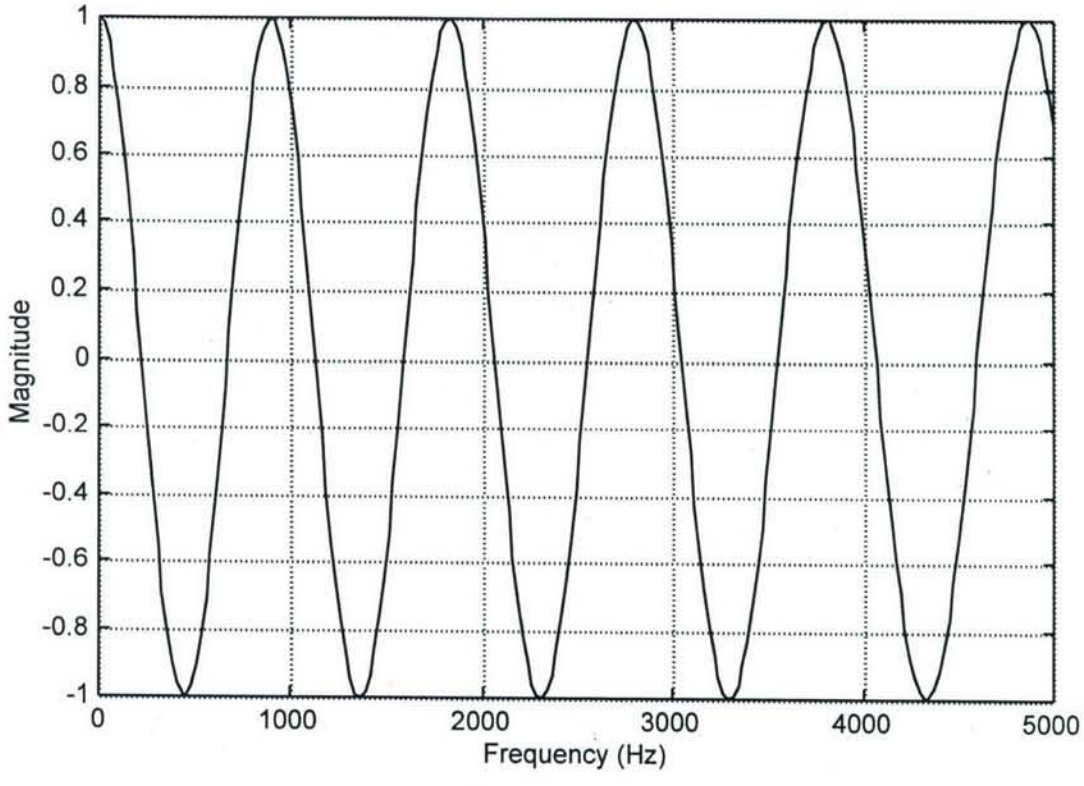
1
0.8
0.6
0.4
0.2
0
-0.2
-0.4
-0.6
-0.8
-1
Magnitude
0
1000
2000
3000
4000
5000
Frequency (Hz)

FIG. 8

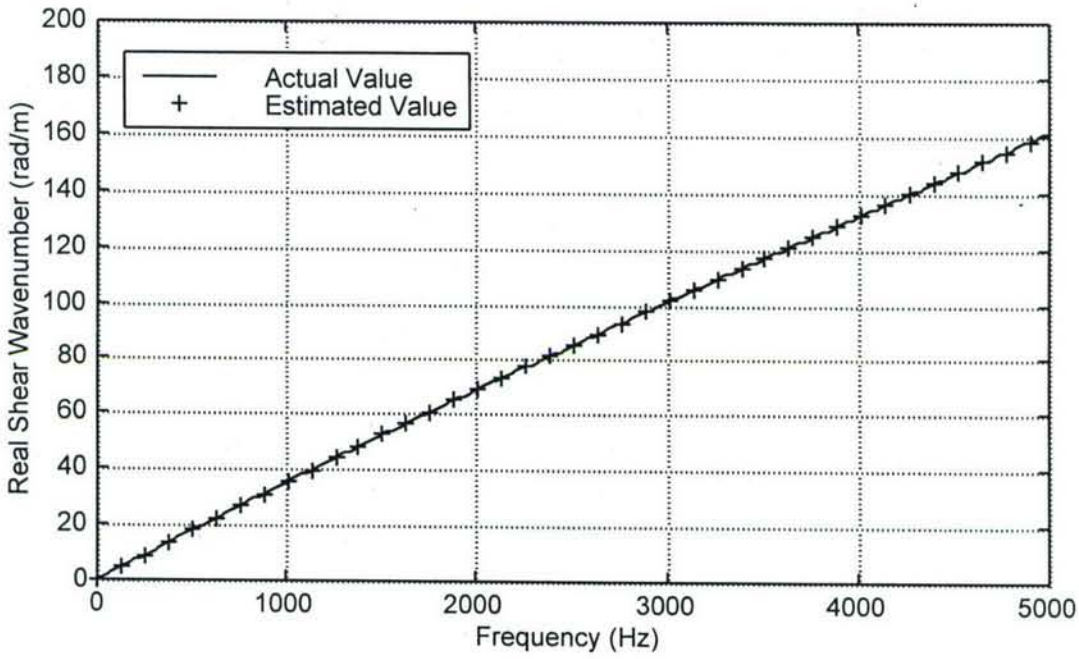
Actual Value
Estimated Value
Real Shear Wavenumber (rad/m)
Frequency (Hz)
0
20
40
60
80
100
120
140
160
180
200
0
1000
2000
3000
4000
5000

FIG. 9A

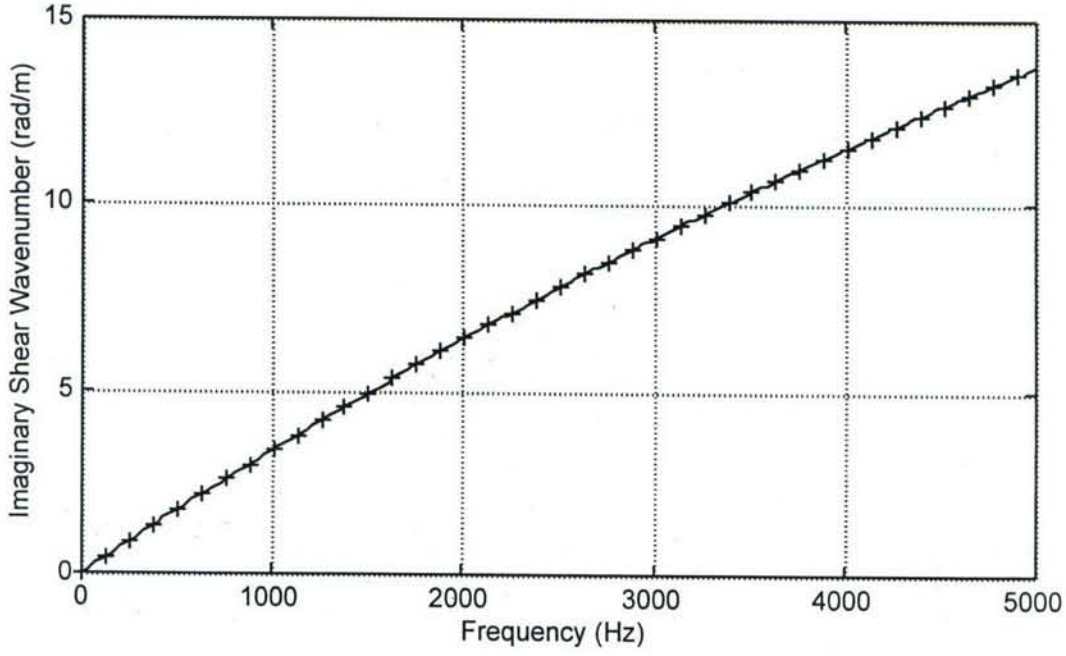
Imaginary Shear Wavenumber (rad/m)
Frequency (Hz)
0
5
10
15
0
1000
2000
3000
4000
5000

FIG. 9B

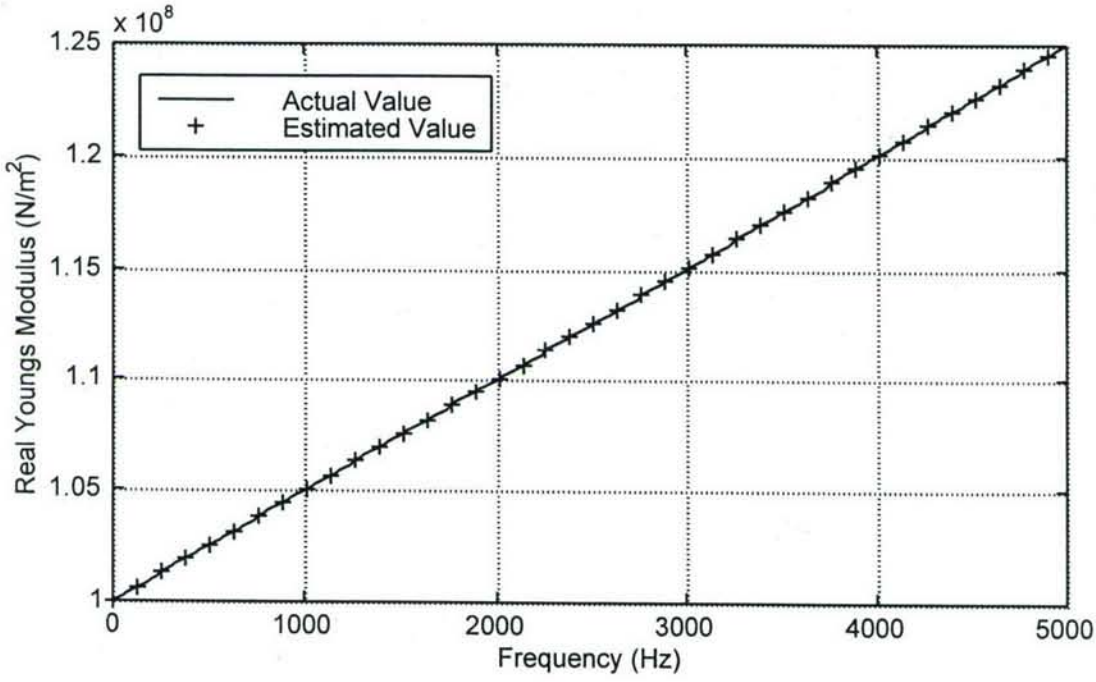

FIG. 10A

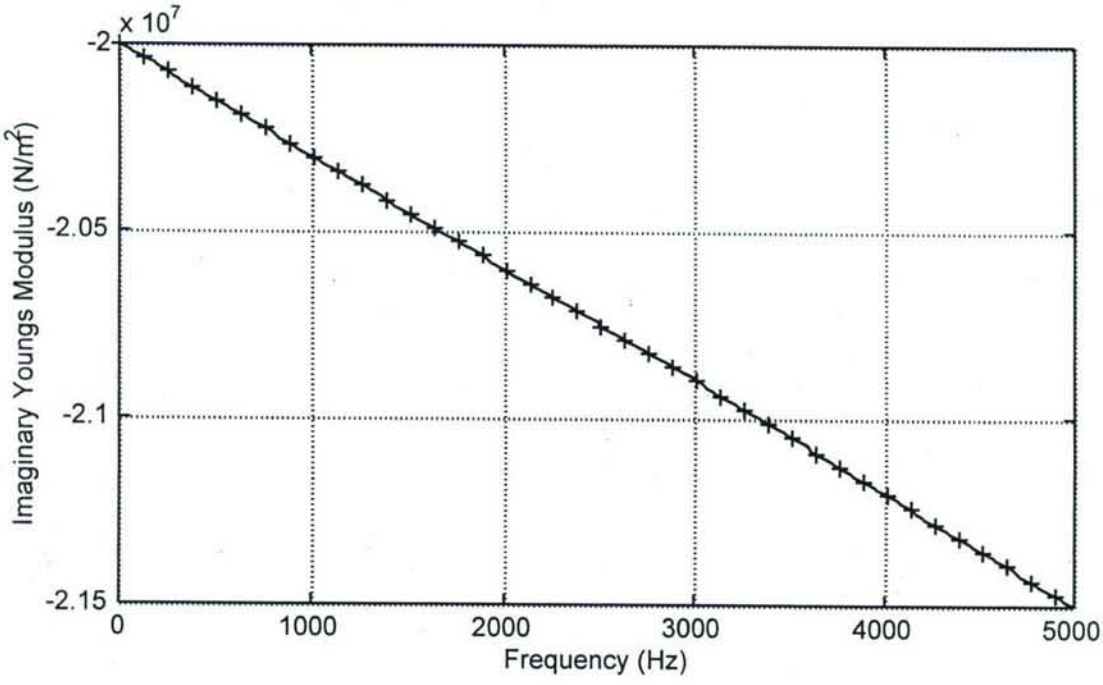

FIG. 10B

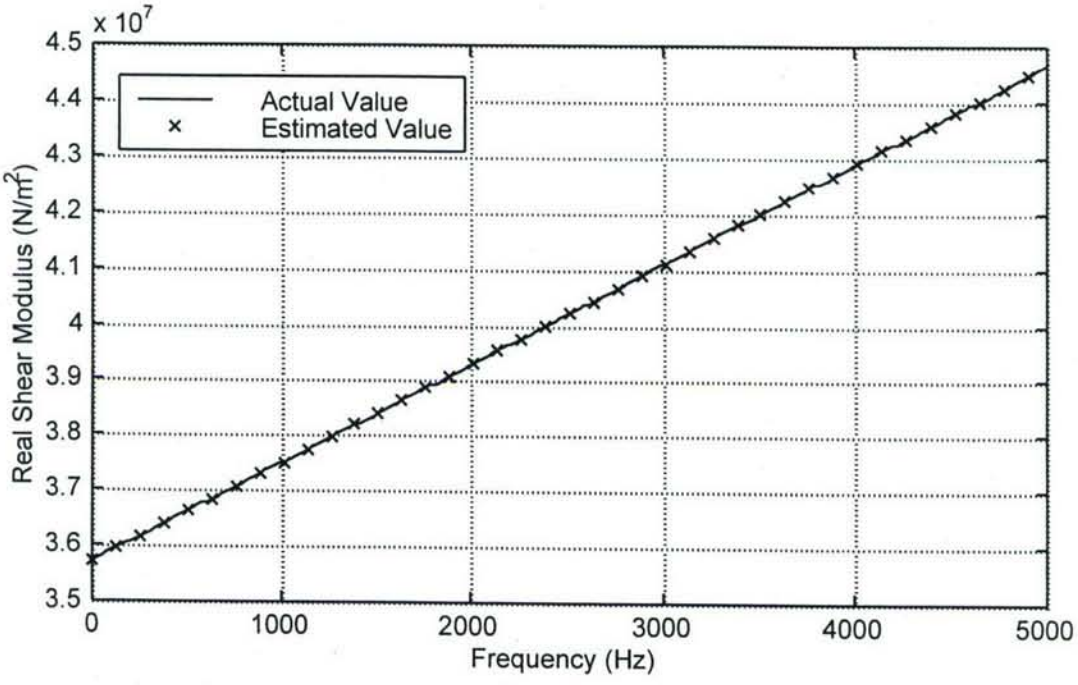

FIG. 11A

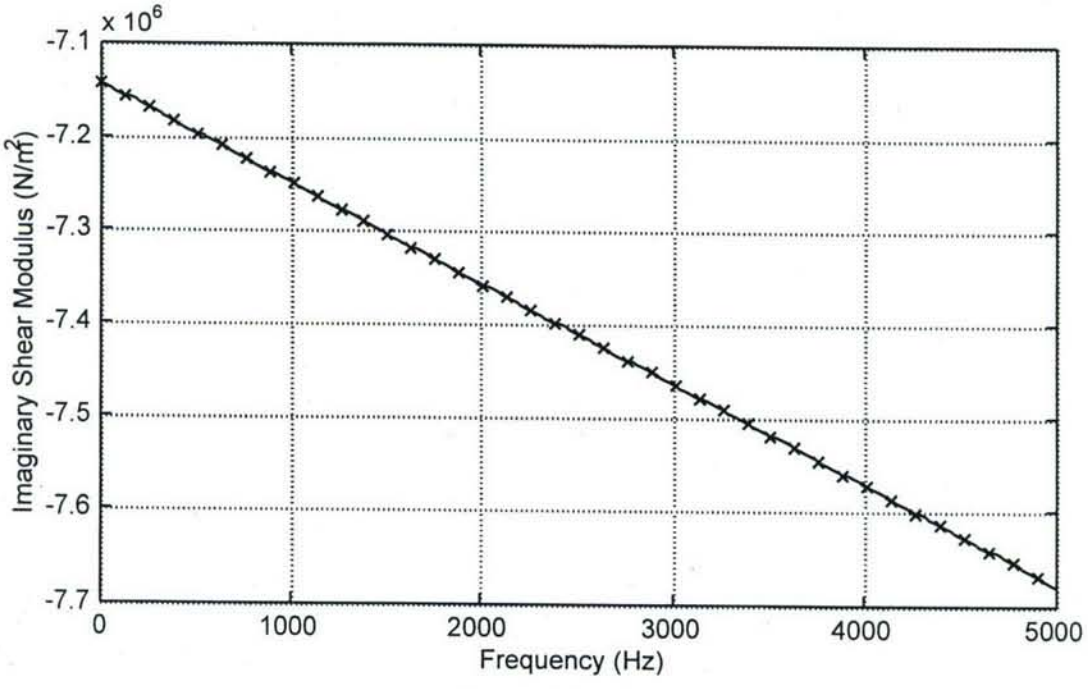

FIG. 11B

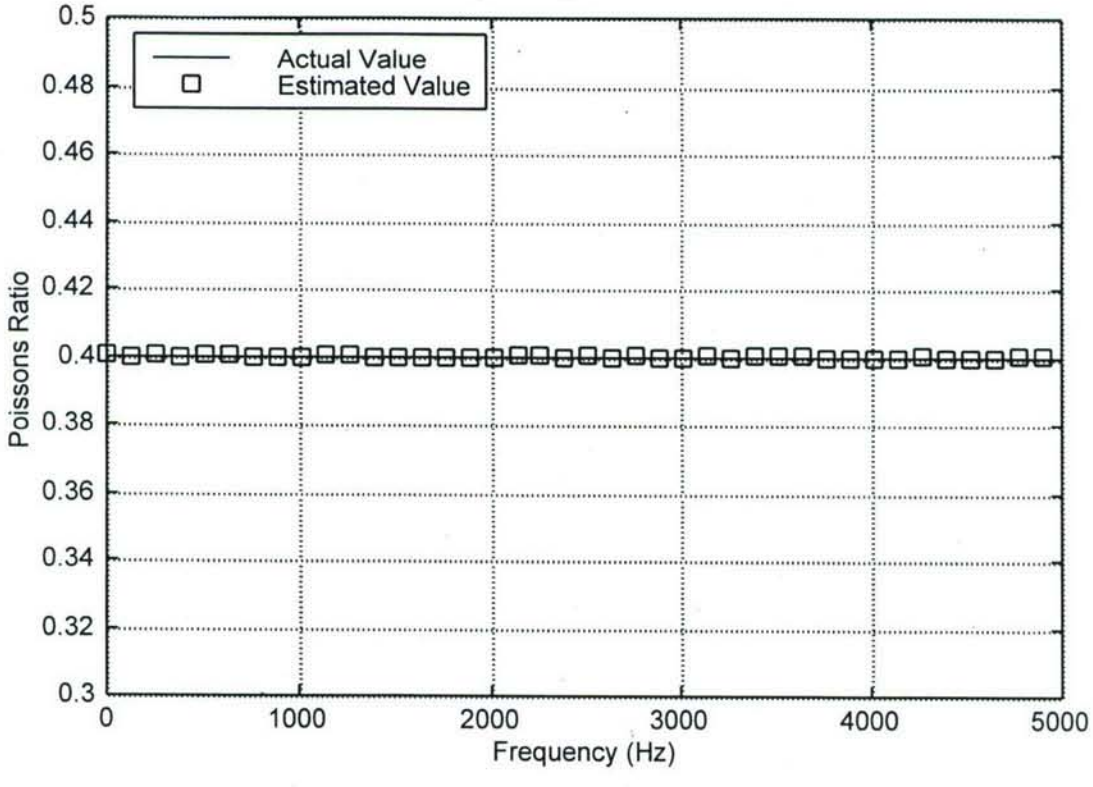
Actual Value
Estimated Value
Poissons Ratio
Frequency (Hz)
0.5
0.48
0.46
0.44
0.42
0.4
0.38
0.36
0.34
0.32
0.3
0
1000
2000
3000
4000
5000

FIG. 12